AIP | Applied Physics Letters

Tailoring the local structure and electronic property of AuPd nanoparticles by selecting capping molecules

Feng Liu and Peng Zhang

Citation: Applied Physics Letters **96**, 043105 (2010); doi: 10.1063/1.3290245
View online: http://dx.doi.org/10.1063/1.3290245
View Table of Contents: http://scitation.aip.org/content/aip/journal/apl/96/4?ver=pdfcov
Published by the AIP Publishing

Tailoring the local structure and electronic property of AuPd nanoparticles by selecting capping molecules

Feng Liu and Peng Zhang[a)]
Department of Chemistry and Institute for Research in Materials, Dalhousie University, Halifax, Nova Scotia, Canada B3H 4J3

(Received 3 October 2009; accepted 16 December 2009; published online 26 January 2010)

Nine AuPd nanoparticle samples selectively capped with tetraoctylphosphonium bromide, primary amine and tertiary amine molecules were studied with the Au L_3-edge x-ray absorption spectroscopy (XAS). The AuPd mixing patterns were analyzed by comparing the XAS results with the theoretical coordination numbers of 24 AuPd model clusters of varied size, Au concentration, and bimetal mixing pattern. It was found that the use of amines, particularly tertiary amine, produced a more homogeneous AuPd mixing pattern and the Au *d*-electron density was fine-tunable by tailoring the density of Au–Pd bonds. Mechanisms for the tailored structural and electronic properties of these nanoparticles were proposed. © *2010 American Institute of Physics*. [doi:10.1063/1.3290245]

Metal nanoparticles (NPs) with well tailored structure and properties have promising applications in areas such as catalysis[1] and biodetection.[2] In order to improve their performance in these applications, preparation of NPs with well controlled bimetallic structure is often desired.[3] Recently, significant advances have been achieved in the preparation of molecularly capped metal NPs.[4] Remarkably, capping molecules also play an important role in tailoring the structure of many metal nanostructures such as nanorods and nanowires.[5] Moreover, selection of the capping molecules has been used to tune the electronic behavior of Au NPs by controlling the metal-capping molecule charge transfer process.[6] Herein we report results on tailoring the bimetallic local structure of AuPd NPs of varied metal concentrations (0.25, 0.50, and 0.75 Au) using selected capping molecules. The NPs were studied by Au L_3-edge extended x-ray absorption fine structure (EXAFS) and x-ray absorption near-edge structure (XANES), which showed that their local structure and electronic behavior can be tailored by selecting the capping molecules.

AuPd bimetallic NPs were prepared using a modified reverse micelle method.[7] Details of the synthesis and purification procedure were presented elsewhere.[8] Three types of capping molecules, tetraoctylphosphonium bromide (TB), primary amine n-dodecylamine (PA), and tertiary amine tri-n-dodecylamine (TA), were selected. The samples were prepared with 100% TB (15TB, 15 referring to the TB-to-Au molar ratio), 80% TB/20% PA (3TB12PA), and 80% TA/20% TB (3TB12TA). The x–ray experiments were performed at the HXMA beamline of Canadian Light Source (CLS). The XAFS data were normalized and fitted using the standard procedure previously described.[8–10] Nonlinear least-squares fit was conducted on the first shell Fourier transformed-EXAFS [k-space range: 3.2 to 13.0 (or 12.5) $Å^{-1}$] by selecting a R window of 1.7–3.3 Å and using the theoretical phase-shift and amplitude functions generated by the FEFF8 program.[11] The AuPd EXAFS model cluster was constructed using lattice parameters from the literature.[12]

Figure 1 shows TEM images of the three series of AuPd NPs capped with 15TB, 3TB12PA, and 3TB12TA. Within each series, three Au concentrations (0.25, 0.50, and 0.75) were used. The average size and standard deviation are provided in Table I. Figure 2 present the experimental and theoretical fit of EXAFS of the three series of NPs. The fitting results of the AuPd samples are provided in Table I.[13] The most useful information on the AuPd local structure comes from the analysis of the coordination number (CN).[3,13,14] The CN of a bulk fcc metal is 12. For monometallic Au NPs, the average CN is less than 12 due to the presence of a large fraction of surface atoms whose CN is less than 12.[8] For the Au L_3-EXAFS fitting results of Au–Pd NPs, two CNs, i.e., CN_{Au-Au} and CN_{Au-Pd}, were obtained. CN_{Au-Au} refers to the average number of Au neighbor atoms and CN_{Au-Pd} to the number of Pd neighbor atoms around the Au absorber. For a homogeneous Au–Pd alloy, the ratio of CN_{Au-Pd}/CN_{Au-Au} should be equal to the Au/Pd molar ratio. The most often encountered nonhomogeneous alloying NPs have a Au

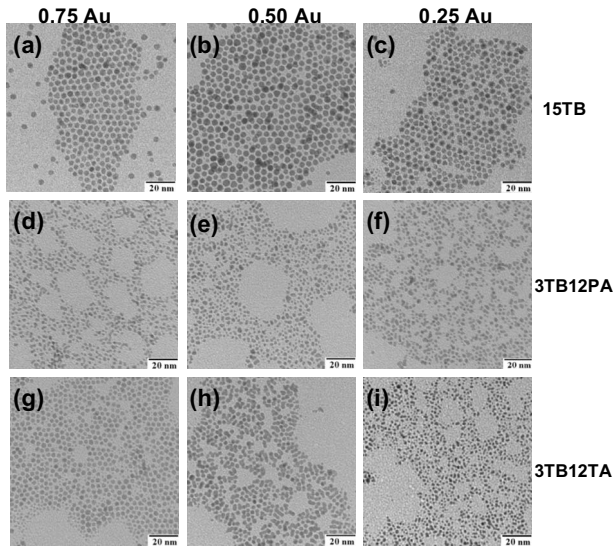

FIG. 1. TEM images of AuPd NPs of varied Au concentrations capped with selected capping molecules. The scale bar is 20 nm in all the images. The Au concentration and types of capping molecules are noted in the figure.

[a)]Author to whom correspondence should be addressed. Tel.: 001-902-4943323. FAX: 001-902-4941310. Electronic mail: peng.zhang@dal.ca.

TABLE I. Structural information of AuPd NPs from EXAFS and TEM.

Samples	Bond	R (Å)	CN	Mixing pattern	CN (model)	Size (nm)
15TB	Au–Au	2.810(4)	8.4(4)	core-shell	11.0	6.4 ± 1.0
$Au_{0.25}Pd_{0.75}$	Au–Pd	2.80(1)	0.7(1)		1.0	
15TB	Au–Au	2.833(2)	6.3(2)	core-shell	10.8	6.3 ± 0.9
$Au_{0.50}Pd_{0.50}$	Au–Pd	2.830(4)	1.4(2)		1.2	
15TB	Au–Au	2.849(5)	7.3(3)	cluster on cluster	···	4.9 ± 1.6
$Au_{0.25}Pd_{0.75}$	Au–Pd	2.84(1)	0.5(1)		···	
3TB12PA	Au–Au	2.843(3)	10.2(3)	core-shell	9.2	3.2 ± 0.9
$Au_{0.75}Pd_{0.25}$	Au–Pd	2.85(1)	1.4(3)		2.1	
3TB12PA	Au–Au	2.808(2)	8.2(4)	core-shell	9.6	3.5 ± 0.9
$Au_{0.50}Pd_{0.50}$	Au–Pd	2.796(5)	2.1(2)		2.4	
3TB12PA	Au–Au	2.780(3)	3.3(2)	inverse cluster on cluster	···	3.3 ± 0.8
$Au_{0.50}Pd_{0.50}$	Au–Pd	2.777(3)	2.5(2)		···	
3TB12TA	Au–Au	2.845(3)	6.3(3)	homoalloy	8.0	4.7 ± 0.9
$Au_{0.75}Pd_{0.25}$	Au–Pd	2.819(4)	2.7(3)		2.6	
3TB12TA	Au–Au	2.822(2)	8.0(3)	core-shell	10.2	4.2 ± 1.0
$Au_{0.50}Pd_{0.50}$	Au–Pd	2.809(3)	1.9(2)		1.8	
3TB12TA	Au–Au	2.777(2)	4.5(2)	random alloy	···	3.2 ± 0.7
$Au_{0.25}Pd_{0.75}$	Au–Pd	2.771(1)	4.3(1)		···	

core—Pd shell structure.[8] In addition, a random alloy structure can be produced if the mixing level of the two metals is considerably higher than that of a core-shell structure but still does not reach the level of a homogeneous alloy. If a second metal is formed mainly on the surface of the first core metal, but only an incomplete shell is formed, a cluster-on-cluster geometry is produced. Overall, for AuPd NPs with identical metal concentrations, the bimetal mixing level (also the ratio of CN_{Au-Pd}/CN_{Au-Au}) increases in the order of cluster-on-cluster <core-shell<random alloy <homogenous alloy.

In order to quantitatively analyze the AuPd mixing pattern using the experimentally determined CNs in Table I, a total of 24 magic-number AuPd model clusters of varied sizes (3.1, 4.2, 5.4, and 6.5 nm), Au concentrations (0.25, 0.50, and 0.75), and bimetal mixing patterns (core-shell and homogeneous alloy) were constructed. Some of the representative model clusters are presented in Fig. 3. Calculation of the CN of a model cluster was performed by weight-averaging the CN of each specific atomic site of the model cluster, illustrated in Fig. 3(b). By comparing the theoretical CNs with the experimental ones, the AuPd mixing patterns were deduced and presented in Table I along with the theoretical CNs of the corresponding model clusters. For the 15TB series, a core-shell structure is assigned to the samples with 0.75 and 0.50 Au due to their similar CNs to that of the corresponding model clusters. The sample with 0.25 Au has a significantly smaller CN_{Au-Pd} than that of its core-shell model cluster (0.5 versus 1.8), indicating that a complete Pd

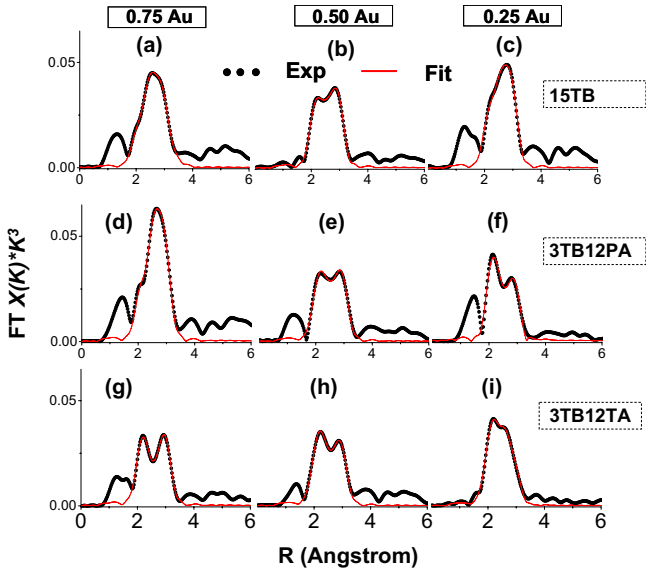

FIG. 2. (Color online) Experimental Au L_3-edge EXAFS and theoretical fits of the nine AuPd samples. The Au concentration and types of capping molecules are also displayed in the figure.

shell was not formed. Therefore, a cluster-on-cluster structure was assigned. For the six amine-protected NPs, three of them (0.75 and 0.50 Au in the 3TB12PA series and 0.50 Au in the 3TB12TA series) are Au core-Pd shell NPs due to the resemblance of their CNs to those of the corresponding core-shell models. The 3TB12PA sample with 0.25 Au has an unusually small CN_{Au-Au} (3.3 versus 8.9 for the core-shell model cluster). Moreover, the CN_{Au-Pd} for this sample (2.5) is far smaller than that of the homogeneous alloy model (CN_{Au-Pd}=7.5). Therefore, the most plausible structure for this sample is an inverse cluster-on-cluster type, that is, very small Au clusters located on a bigger Pd cluster, distinguished from the cluster-on-cluster structure in the 15TB series where small Pd clusters are on a bigger Au cluster.[8] The 3TB12TA sample with 0.75 Au has CNs very close to those of the corresponding homogeneous alloy model (CN_{Au-Au}/CN_{Au-Pd}:6.3/2.7 versus 8.0/2.6), indicating a nearly homogeneous alloy structure. The CNs of the 3TB12TA sample with 0.25 Au is in between those of a core-shell and a homogeneous alloy model (CN_{Au-Au}/CN_{Au-Pd}:4.5/4.3 for the sample versus 8.9/3.1 for the core-shell and 2.5/7.5 for the homogeneous alloy model). Thus a random alloy structure is indicated. It must be noted that, strictly speaking, these two 3TB12TA samples are both random alloy in nature. However, since the CNs of the 0.75 Au sample is much closer to those of a homogeneous alloy (i.e., it is a nearly homogeneous alloy), we use the term "homoalloy" in Table I for this sample to emphasize its significantly higher AuPd mixing level than the other random alloy sample (3TB12TA with 0.25 Au).

By considering the results on the NP bimetal mixing level, it is evident that the use of amine capping molecules, particularly the tertiary amine, leads to a more homogeneous bimetallic mixing pattern (i.e., increased ratio of CN_{Au-Pd}/CN_{Au-Au}); whereas in the absence of amines the least mixing level is resulted. This trend is particularly obvious for the three 0.75 Au NPs. Indeed, the 15TB sample (0.75Au) represents the least homogeneous bimetallic mixing (i.e., least Au–Pd bonds per unit volume) whereas the

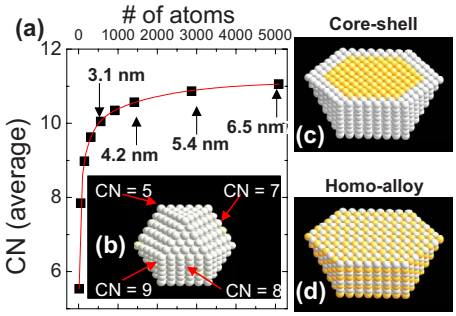

FIG. 3. (Color online) (a) A plot of CN vs number of atoms in the magic-number model clusters (square) and the third-order exponential decay fit (line); (b) An illustration of the CN of each type of surface atoms of the model cluster; [(c) and (d)] Schematic illustrations of the 4.2 nm AuPd model clusters with a core-shell (c) and a homogeneous alloy (d) structure used for the theoretical calculations.

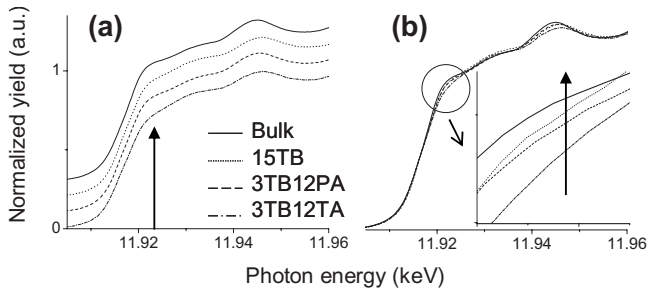

FIG. 4. The Au L_3–XANES displayed by vertically shifting the spectra to compare the profiles (a) and without vertical shift to compare the white line intensity (b).

3TB12TA sample (0.75 Au) has the most homogeneous mixing. The 3TB12PA sample (0.75 Au) lies in between the above two samples in regard to the homogeneity of AuPd mixing pattern.

It has been reported that amines can interact with gold compound to form amine-gold complexes which can be used subsequently to prepare Au NPs.[15,16] It has also been well known that one important reason for the formation of non-homogeneous AuPd NPs is that Au compounds can often reoxidize the reduced Pd(0), leading to the formation of bigger Au clusters prior to the reduction of Pd.[17] Therefore, it seems plausible that the amine-gold complex is less efficient in the redox reaction with Pd(0), resulting in a slower formation of Au(0) during the formation of AuPd NPs. This notion also well interprets why the use of tertiary amine can lead to an even more homogeneous AuPd mixing pattern (e.g., the homogeneous alloy structure for the 0.75 Au sample). That is, the more bulky tertiary amines should make the amine-gold complex even less efficient in reacting with Pd(0).

Based on the tailored structure associated with the three capping molecules, we illustrate the fine-tunable electronic property of the NPs using the three 0.75 Au NPs with representative bimetal mixing level. Figure 4 is the Au L_3-edge XANES of the AuPd NPs and bulk Au. The small peak right after the edge jump, known as the white line, corresponds to the electronic transition from $2p$ to unoccupied $5d$ states.[18] An increased white line corresponds to more unoccupied $5d$ states (d-hole) or less $5d$-electrons. In Fig. 4(a), the spectral shapes of the three AuPd samples and bulk Au are compared; in Fig. 4(b), the white lines of the samples are more closely compared by aligning the Fermi levels of the NPs with that of the bulk. It is found that the white line intensity decreases in the order of bulk > 15TB > 3TB12PA > 3TB12TA. This observation is consistent with the trend of increasing Au–Pd bond density in the NPs. The observation in Fig. 4(b) is also in good agreement with our previous theoretical results.[8] The AuPd alloying interaction is the main factor in determining the d-electron density of the three NPs. The NPs with the highest density of Au–Pd bonds (homogeneous alloy) thus show the highest d-electron density and the NPs with the lowest density of Au–Pd bonds (15TB) have the lowest d-electron density. These results provide clear evidence that the tailored bimetallic mixing patterns can lead to a fine-tuning of the d-electron density of Au atoms. This finding should be useful in designing Au-based catalysts and electronic devices.

In summary, we have reported that by selecting three types of capping molecules the bimetallic mixing pattern of AuPd NPs can be possibly tailored, which was revealed by Au L_3-edge EXAFS. The Au L_3-edge XANES data indicate that the d-electron density of Au atoms can be tuned by tailoring the bimetallic mixing patterns. Mechanisms on the tailored structural and electronic properties of the NPs were also proposed.

This work is financially supported by Dalhousie University and NSERC Canada. The infrastructure of laboratory research facilities are supported by CFI. The Canadian light source (CLS) is supported by NSERC, CIHR, NRC and the University of Saskatchewan. We acknowledge the CLS staff scientist Dr. Ning Chen (HXMA beamline) for the synchrotron technical support.

[1] A. Roucoux, J. Schulz, and H. Patin, Chem. Rev. **102**, 3757 (2002).
[2] M. C. Daniel and D. Astruc, Chem. Rev. (Washington, D.C.) **104**, 293 (2004).
[3] R. Ferrando, J. Jellinek, and R. L. Johnston, Chem. Rev. (Washington, D.C.) **108**, 845 (2008).
[4] J. A. Dahl, B. L. S. Maddux, and J. E. Hutchison, Chem. Rev. (Washington, D.C.) **107**, 2228 (2007).
[5] C. J. Murphy, T. K. San, A. M. Gole, C. J. Orendorff, J. X. Gao, L. Gou, S. E. Hunyadi, and T. Li, J. Phys. Chem. B **109**, 13857 (2005).
[6] P. Zhang and T. K. Sham, Appl. Phys. Lett. **81**, 736 (2002).
[7] M. Brust, M. Walker, D. Bethell, D. J. Schiffrin, and R. Whyman, J. Chem. Soc., Chem. Commun. **801** (1994).
[8] F. Liu, D. Wechsler, and P. Zhang, Chem. Phys. Lett. **461**, 254 (2008).
[9] P. Zhang, P. S. Kim, and T. K. Sham, Appl. Phys. Lett. **82**, 1470 (2003).
[10] P. Zhang and T. K. Sham, Appl. Phys. Lett. **82**, 1778 (2003).
[11] A. L. Ankudinov, B. Ravel, J. J. Rehr, and S. D. Conradson, Phys. Rev. B **58**, 7565 (1998).
[12] A. Maeland and T. B. Flanagan, Can. J. Phys. **42**, 2364 (1964).
[13] R. J. Davis and M. Boudart, J. Phys. Chem. **98**, 5471 (1994).
[14] A. I. Frenkel, C. W. Hills, and R. G. Nuzzo, J. Phys. Chem. B **105**, 12689 (2001).
[15] S. Gomez, K. Philippot, V. Colliere, B. Chaudret, F. Senocq, and P. Lecante, Chem. Comm. (Cambridge) **2000**, 1945.
[16] M. Aslam, L. Fu, M. Su, K. Vijayamohanan, and V. P. Dravid, J. Mater. Chem. **14**, 1795 (2004).
[17] N. Toshima and T. Yonezawa, New J. Chem. **22**, 1179 (1998).
[18] P. Zhang and T. K. Sham, Phys. Rev. Lett. **90**, 245502 (2003).